



Theoretical study on the formation of diamond germanium vacancy color center

Xin Tan^{*}, Wei Shao, Xiyu Ma, Zanqing He, Bochen Zhang, Chengbin Chen, Yuan Ren, Shiyang Sun

School of Mechanical Engineering, Inner Mongolia University of Science & Technology, Baotou, Inner Mongolia 014010, PR China

ARTICLE INFO

Keywords:

First-principles method
Germanium doping
Adsorption energy
Diamond surfaces

ABSTRACT

Germanium-vacancy (GeV) color centers in diamond are superior to other color centers in terms of luminescence intensity. The Ge-doping process is key to the successful preparation of GeV color centers in diamond. In this study, the formation mechanism of GeV color centers is explored via first-principles calculations of the adsorption and migration of Ge on the (001) surface of diamond. The results reveal that Ge atoms on the surface of completely hydrogenated diamond have a negative adsorption energy, indicating that they cannot be adsorbed. In contrast, the adsorption energy of Ge atoms on the surface of non-perhydrogenated diamond is relatively large, which indicates that the surface of non-perhydrogenated diamond can adsorb Ge atoms. When Ge atoms are closer to hydrogen defects, their adsorption energy is greater. As the extent of hydrogen deficiency increases, the overall adsorption energy increases accordingly. The hydrogen deficiency of the diamond surface may determine the extent of the Ge content on the diamond surface. Magnetic moment, differential charge, and Bader analyses reveal that charge is transferred between Ge and carbon atoms on the diamond surface. In addition, the Ge and carbon atoms form covalent bonds at positions where the adsorption energy is maximum. Finally, the migration of Ge atoms on the diamond surface enables them to reach a stable position easily.

1. Introduction

Owing to its excellent physical properties, stable chemical properties, and internal defects at room temperature, diamond continues to attract the attention of researchers from a variety of fields. Color centers in diamond, which comprise impurity atoms and lattice holes, are characterized by their stable single-photon emission and easy spin manipulation at room temperature. Combined with the advantages of diamond itself, such as high stability, strong acid and alkali resistance, and biological compatibility [1], such color centers have shown great application value in the fields of quantum information processing, quantum sensing, biomarkers, and high-resolution imaging [2–4].

Diamond color centers exhibit narrow line widths, and different diamond color centers fluoresce at different wavelengths. Owing to their narrow spectral width and short fluorescence lifetimes [5], germanium-vacancy (GeV) color centers demonstrate a higher quantum photoluminescence efficiency than their silicon-based counterparts. As such, GeV color centers are effective quantum emitters for nanophotonic devices [6], with their enhanced quantum efficiency helping to improve

the temperature and spatial resolution of nanoscale temperature measurements [7]. The zero-phonon line (ZPL) of GeVs occurs at 602 nm and exhibits D3d symmetry with silicon-vacancy (SiV) color centers [8]. Moreover, GeVs have a higher ground-state splitting value than SiVs, resulting in a relatively long spin coherence time [9]. These features make GeV color centers attractive for many applications in the field of quantum optics, including single-photon emission [6,10] and temperature sensing [11].

At present, GeV color centers in diamond are typically prepared using either chemical vapor deposition (CVD) [12] or ion implantation [13]. While ion implantation can provide more accurate positioning of the color centers, it damages the crystal structure of diamond, with even high-temperature annealing unable to eliminate the problem of residual radiation damage [13]. In contrast, CVD produces uniformly distributed GeV color centers without destroying the diamond crystal structure [14]. The main principle of the CVD-based Ge doping of diamond films is the adsorption of Ge atoms on the surface of the diamond as it is deposited during film growth. Therefore, to form Ge-doped diamond, Ge atoms are first adsorbed on the diamond surface before migrating to a

* Corresponding author: Arding Str. No. 7, Baotou, Inner Mongolia, 014010, PR China.

E-mail address: heart_tan@126.com (X. Tan).

stable position. The total adsorption energy of Ge at various positions on the diamond surface determines whether Ge atoms are adsorbed stably. Ultimately, the adsorption energy affects the extent of the Ge doping and, subsequently, the number of GeV color centers. This study uses the first-principles approach to analyze the adsorption and migration of Ge on the surface of diamond during the CVD process. The main objective of this work is to elucidate the Ge-doping mechanism and thus provide theoretical guidance for the optimal preparation of GeV color centers.

2. Calculation method and model

The first-principles method was implemented using VASP software [15–17], and uses plane waves and periodic boundary conditions to perform density functional theory calculations. The interactions between electrons and ions were represented by the projector augmented wave (PAW) method [18,19], with the local electron density expressed by the Perdew–Burke–Ernzerhof (PBE) functional in the generalized gradient approximation (GGA) [20,21]. The Monkhorst–Pack scheme [22] was used to represent the k-point of the Brillouin zone ($5 \times 5 \times 1$), which has a cutoff at 350 eV. Using spin polarization, the electron and ion relaxation convergence accuracies were determined to be 10–4 eV and 10–3 eV, respectively, while the migration of Ge atoms on the diamond surface was calculated using the nudged elastic band (NEB) method [23]. The theoretical model of diamond, comprising $4 \times 4 \times 8$

carbon atoms, is shown in Fig. 1. The upper and lower surfaces of the diamond both possess 4×4 hydrogen atoms, with the vacuum layer measuring 1.28 nm in height. Because H⁺ ions are involved in the CVD-based preparation of diamond films, the hydrogen termination interface is also the deposition interface. To calculate the accuracy of the adsorption and migration, the hydrogen termination model was relaxed and reconstructed to obtain the dimer structure. Fig. 1 shows the high-symmetry positions, ①–⑥, after reconstruction: ① dimer bridge position (P1); ② the top position of the first carbon atom (P2); ③ dimer open ring bridge position (P3); ④ dimer chain open ring gap (P4); ⑤ dimer line open ring gap (P5); ⑥ dimerization bulk chain closed loop gap (P6). For the adsorption calculations, Ge atoms are placed above each of these high-symmetry sites.

By reducing the number of hydrogen atoms at different positions, as shown in Fig. 1(c), eight different hydrogen-deficient diamond surfaces can be obtained: when position B lacks a hydrogen atom, an open radical site (1ORS) is generated; when positions B and E both lack a hydrogen atom, two open radical sites (2ORS-CC) are created on the closed ring side of the dimer chain; when positions B and C lack a hydrogen atom, position C produces two open radical positions on the open side of the dimer chain (2ORS-CO); when positions A and B lack hydrogen atoms, two open radical positions are produced in the direction of the dimer (2ORS-R); when the hydrogen atoms are lacking at positions A, B, and D simultaneously, three open radicals (3ORS-R) are generated in the

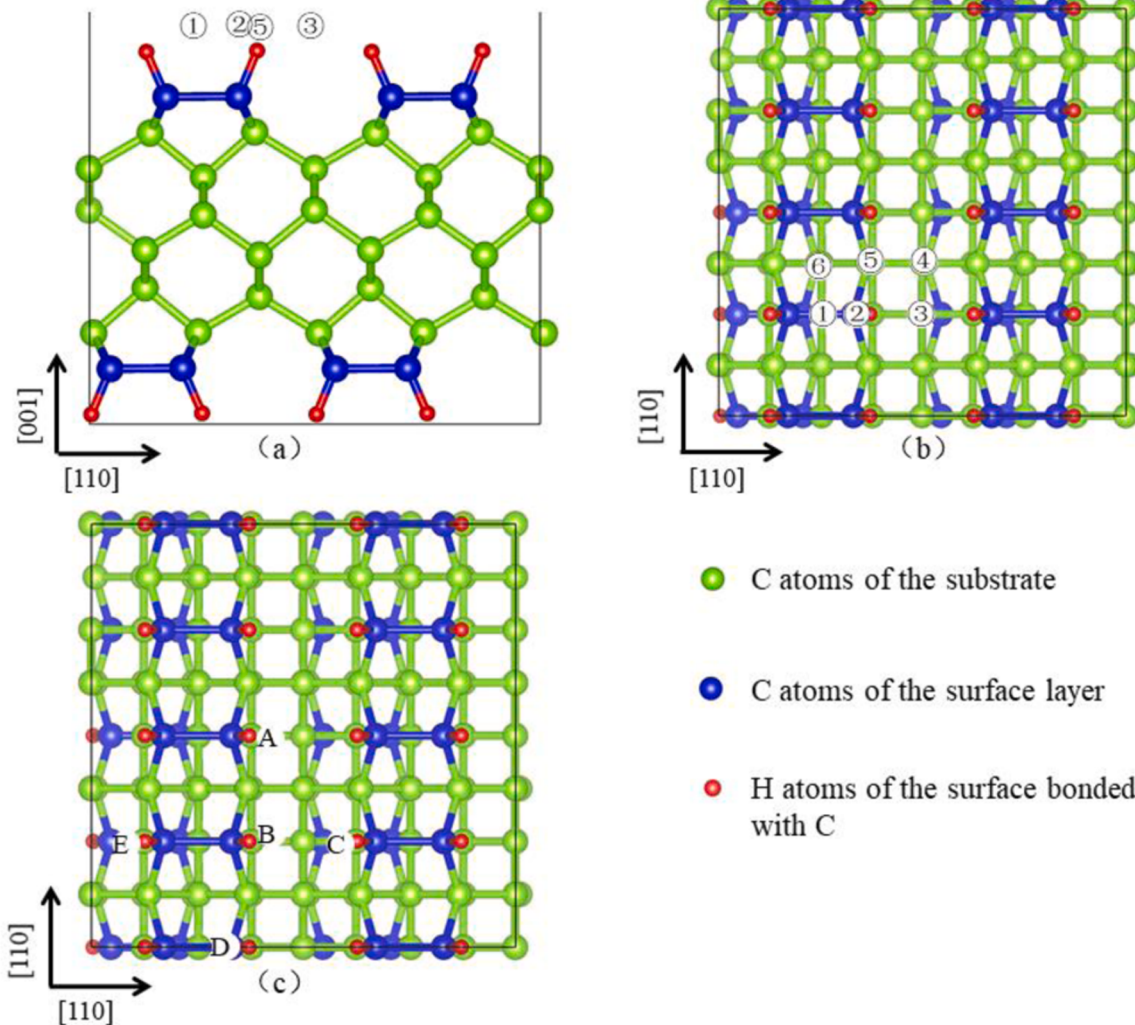


Fig. 1. Surface model of the (001) plane of completely hydrogen-terminated diamond: (a) front view of the six high-symmetry sites, (b) top view of the six high-symmetry sites, and (c) hydrogen-terminated defect sites.

direction of the dimer; when hydrogen atoms are lacking at positions E, B, and C concurrently, three open free radicals (3ORS-C) are created in the direction of the dimer chain [24]; when there are no open free radicals on the diamond surface, it is completely hydrogen terminated (NORS); non hydrogen-terminated diamond surfaces are considered clean (Diamond).

In order to verify the rationality of the model, parts of the established models were expanded to different degrees, then we did the calculation. The calculation results were compared with those of the model in this paper, and the error was within a reasonable range. Therefore, the model built in this paper is reasonable.

First, the single-atom energies of diamond and Ge were calculated as -1.48 eV [25] and -0.767 eV, respectively. To ensure the accuracy of the calculation, the lattice constant and binding energy in the calculation were compared with experimental values [26]. The lattice constant errors of Ge and diamond were calculated as 2.131% and 0.03% , respectively. In addition, the respective binding energy errors were calculated as 3.223% and 3.47% . These values all lie within acceptable error margins.

3. Analysis and discussion

The adsorption energy of the Ge atoms at the six high-symmetry sites was calculated using the following expression [24]:

$$Ead = -(E_{tot} - E_{slab} - nEGe) \quad (1)$$

where Ead is the total adsorption energy of the Ge atoms at the corresponding high-symmetry position, E_{tot} is the total energy of the configuration of Ge atoms at the corresponding high-symmetry position, E_{slab} is the total energy of the configuration of diamond models without Ge atoms, n is the number of adsorbed Ge atoms, and EGe is the single-atom energy of Ge atoms.

3.1. Adsorption behavior of Ge atoms on the diamond surface

First, we analyzed the stability of the adsorption of Ge atoms on the diamond surface from the perspective of bond length and type. The adsorption energies of Ge atoms on various diamond surfaces were calculated using Formula 1, with the results listed in Table 1. The adsorption energy on the surface of the perhydrogen-terminated diamond is negative at each of the six high-symmetry positions. It can be seen from Table 2 that the distance separating Ge and C atoms is far greater than the sum of their covalent bond radii (0.199 nm). This indicates that the Ge atoms are completely desorbed when the diamond is terminated by hydrogen. This may be due to the bonding of H and C atoms on the surface of the diamond, with hydrogen termination saturating their electron pairs. Consequently, there are no spare electrons to bond with Ge atoms, preventing their adsorption on the hydrogen-terminated surface and restricting the Ge doping concentration.

When a hydrogen defect appears on the diamond surface, an active site appears on the C atom at the corresponding hydrogen-deficient position. The adsorption energy of the corresponding 1ORS in Tables 1 and 2 is inversely proportional to the bond length. When the

Table 1
Adsorption energy of germanium atoms in various diamond models.

Ead (eV)	P1	P2	P3	P4	P5	P6
NORS	-0.528	-0.504	-0.549	-0.581	-0.544	-0.609
1ORS	1.771	2.179	1.281	0.226	1.254	0.335
2ORS-CC	4.06	3.438	1.079	0.529	1.779	2.498
2ORS-CO	1.356	1.982	4.162	2.152	1.398	-0.019
2ORS-R	1.776	2.562	1.392	2.137	4.075	2.637
3ORS-C	3.025	2.454	3.314	1.426	0.913	1.442
3ORS-R	2.162	3.125	1.843	2.353	4.306	2.845
Diamond	3.516	3.074	2.348	2.101	2.461	2.855

Table 2
Bond lengths of Ge atoms adsorbed on various diamond surfaces.

C-Ge bond length (nm)	P1	P2	P3	P4	P5	P6
NORS	0.305	0.305	0.341	0.374	0.333	0.356
1ORS	0.213	0.202	0.241	0.297	0.228	0.259
2ORS-CC	0.204	0.197	0.252	0.350	0.227	0.227
2ORS-CO	0.212	0.201	0.218	0.248	0.222	0.248
2ORS-R	0.210	0.198	0.235	0.248	0.209	0.221
3ORS-C	0.205	0.197	0.219	0.254	0.227	0.227
3ORS-R	0.210	0.197	0.234	0.247	0.209	0.221
Diamond	0.205	0.197	0.222	0.254	0.215	0.234

adsorption energy increases, the bond length decreases accordingly, becoming closer in length to the covalent bond radius. The maximum adsorption energy (2.179 eV) occurs at P2, corresponding to the nearest-carbon bond length of 0.202 nm (see Fig. 2(a)), which is close to the sum of the Ge/C covalent bond radius. However, because of the small adsorption energy at P6 and P4, although the adsorption energy is positive, the Ge and C atoms only undergo simple physical adsorption [27] and do not form chemical bonds. Combined with Fig. 1, this suggests that the distance between Ge atoms and the active site influences the size of the adsorption energy: when the distance between Ge atoms and the active site is smaller, the adsorption energy is larger. This is supported by the fact that the distance between Ge atoms and active sites is largest at positions P6 and P4. The adsorption capacity of Ge at P2 is the closest to the defect position, resulting in the maximum adsorption energy.

The adsorption energy and bond length corresponding to the situation where two hydrogen defects are present on the (001) surface of diamond are listed in Tables 1 and 2. For the 2ORS-CC model, the maximum adsorption energy (4.06 eV) occurs at P1. The Ge atom forms a bond with the two surrounding C atoms, resulting in bond lengths of 0.204 nm and 0.205 nm, as shown in Fig. 2(b). The maximum value of the secondary adsorption energy (3.438 eV) is at P2. In this case, the Ge atom bonds only to one neighboring C atom (bond length: 0.197 nm). The bond lengths at P1 and P2 are very close to the covalent bond radius. Because the Ge atom only bonds with one C atom at position P2, the adsorption energy and stability are smaller than at P1. The maximum adsorption energy (4.162 eV) for the 2ORS-CO model is located at P3. The Ge atom bonds to two C atoms with bond lengths of 0.218 nm and 0.220 nm. In addition, the peak secondary adsorption energy (2.152 eV) occurs at P4, with bond lengths of 0.248 nm and 0.250 nm. The maximum adsorption energy (4.075 eV) for the 2ORS-R model is at P5. Here, the Ge atom forms bonds with two surrounding C atoms, both of which measure 0.209 nm, as shown in Fig. 2(d), which is close to the covalent bond radius. The maximum second adsorption energy (2.367 eV) occurs at position P6, with both bonds measuring 0.221 nm.

Comparing the surface of 2ORS-CC with that of 2ORS-CO, it can be seen that the maximum adsorption energy of the 2ORS-CO surface is slightly larger than that of the 2ORS-CC surface. Because there is no C—C bond at the ring-opening position, the larger gap between the C atoms facilitates the adsorption of Ge atoms. On the 2ORS-CC surface, the maximum adsorption energy coincides with the center of the hydrogen defect rather than the gap position of the dimer ring opening. This indicates that Ge atoms are adsorbed more easily at locations with suspended bonds. Comparing the surfaces of 2ORS-CO and 2ORS-CC reveals that the maximum adsorption energy of the 2ORS-CO surface is slightly larger than that of the 2ORS-CC surface; however, the bond of the 2ORS-CC length is slightly shorter. It is possible that the differing properties of these diamond surfaces are due to the different positions of the maximum adsorption energy and the different positions of the hydrogen deficiency, which affects the influence of the surrounding C atoms on the Ge atoms. Consulting Table 2 indicates that the desorption phenomenon observed for the 2ORS-CO surface at position P6 may be caused by the interaction of atoms on the diamond surface. The desorption of Ge atoms occurs when the repulsive force between the

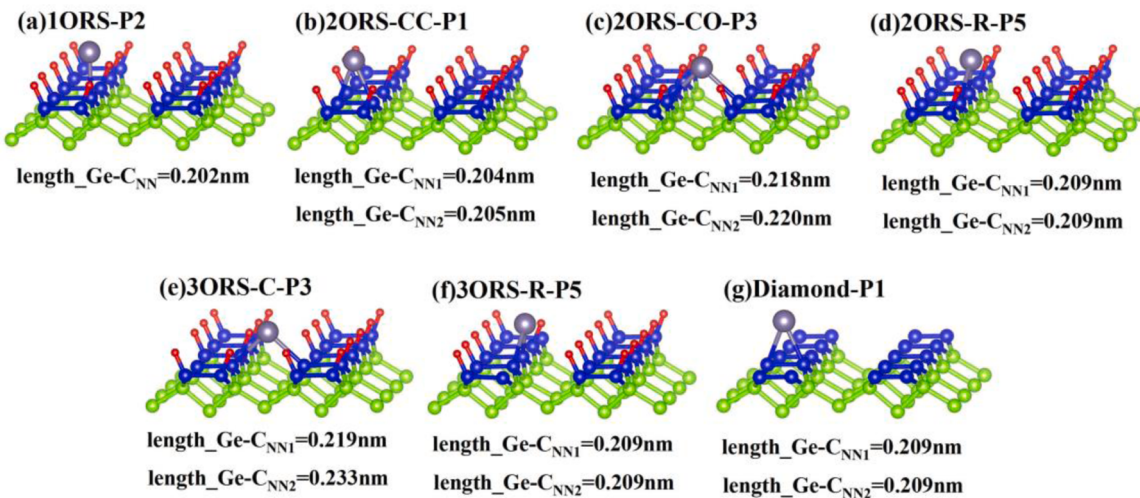


Fig. 2. Bond lengths at the position of maximum adsorption energy regarding the adsorption of Ge on various types of diamond surfaces.

atoms on the surface exceeds the attractive force. The maximum adsorption energy of the 2ORS diamond surface is larger than that of the 1ORS diamond surface. For the 2ORS case, because the Ge atoms form bonds with two C atoms simultaneously, they can be adsorbed more stably on the diamond surface.

The adsorption energies and bond length of the 3ORS-C diamond surface, which contains three hydrogen termination defects, are shown in Tables 1 and 2, respectively. The maximum adsorption energy (3.314 eV) occurs at P3, corresponding to Ge-C bond lengths of 0.219 nm and 0.233 nm (Fig. 2(e)). In contrast, the secondary adsorption energy (3.025 eV) is at P1, corresponding to bond lengths of 0.205 nm and 0.206 nm. Upon comparing positions P1 and P3 in Fig. 1, it is evident that the C atoms either side of the Ge atom have dangling bonds. Nevertheless, each position has distinct features: P3 is an open-ring bridging position, where the larger interatomic gap may cause a larger adsorption energy, whereas P1 is a closed-loop bridging position, where the smaller interatomic gap results in the force between the atoms exceeding that at P3. Therefore, although there are dangling bonds on both sides of the P1 and P3 positions, the adsorption energy at P3 is greater than that at P1, while the bond length at P1 is greater than that at P3. The maximum surface adsorption energy of 3ORS-R (4.306 eV) occurs at P5. The Ge-C bond lengths are 0.209 nm and 0.210 nm (Fig. 3(f)). The maximum secondary adsorption energy (3.125 eV) occurs at P2, with a corresponding bond length of 0.197 nm, which is extremely close to the sum of the covalent bond radii of the Ge atoms and C atoms (0.199 nm). The results for the 3ORS-C and 3ORS-R surfaces indicate that, from the perspective of the total number of hydrogen defects, as the number of hydrogen defects increases, the adsorption energy gradually increases.

The adsorption energies and bond lengths for the case where there is no hydrogen termination on the diamond surface (denoted as the “Diamond” surface) are also listed in Tables 1 and 2. The maximum adsorption energy of Ge atoms occurs at the P1 position and has a value of 3.516 eV, with corresponding Ge-C bond lengths of 0.205 nm and 0.206 nm (Fig. 3(g)). The secondary adsorption energy (3.074 eV) occurs at P2, where the bond length is 0.197 nm. The minimum adsorption energy of the hydrogen-free diamond surface is 2.101 eV, which is substantially larger than the minimum adsorption energy of other diamond surfaces. This is attributed to the influence of hydrogen atoms on Ge adsorption not being a factor for the hydrogen-free terminated diamond. As such, the Ge atoms are free to bond with neighboring C atoms. Therefore, to improve the adsorption of Ge on the diamond surface and increase the doping probability when preparing Ge-doped diamond, the formation of hydrogen on the termination surface should be minimized.

3.2. Bader analysis and magnetic moments of germanium atoms adsorbed on the diamond surface

To verify our explanation of the Ge adsorption on diamond surfaces in Section 3.1, this section uses charge transfer and magnetic moment calculations as the basis for a quantitative analysis of the Ge adsorption mechanism. Fig. 3 shows the differential charge diagrams for the maximum adsorption energy positions of the different hydrogen-terminated diamond surfaces, while Table 3 lists the corresponding charge transfer and magnetic moment values. In Fig. 3, red electron clouds in the differential charge diagrams represent regions of electron gain, while blue clouds indicate regions of electron loss. It is clear that Ge and C atoms both experience electron migration, with the electron

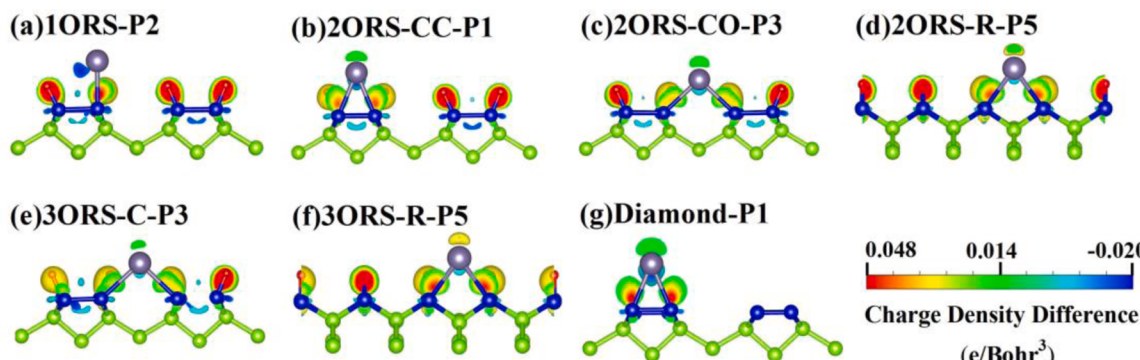


Fig. 3. Differential charges of Ge atoms after adsorption on different hydrogen-terminated diamond surfaces.

Table 3

Bader charge transfers and magnetic moments of Ge atoms before and after adsorption on different diamond surfaces.

		Before adsorption		After adsorption	
		Charge (e)	Magnetic moment (μB)	Charge (e)	Magnetic moment (μB)
1ORS	CNN	4.104	0.386	4.324	-0.015
	Ge	3.960	-0.773	3.592	0.371
2ORS-CC	CNN1	4.05	0.338	4.253	0.00
	CNN2	4.193	0.391	4.437	0.00
2ORS-CO	Ge	3.942	-0.781	3.354	0.00
	CNN1	4.145	0.404	4.309	0.00
2ORS-R	CNN2	4.120	0.408	4.286	0.00
	Ge	4.008	-0.775	3.320	0.00
3ORS-C	CNN1	4.134	0.418	4.30	0.00
	CNN2	4.033	0.00	4.039	0.00
3ORS-R	Ge	4.020	-0.779	3.302	0.00
	CNN1	4.105	0.4	4.279	0.00
Diamond	CNN2	4.199	-0.003	4.253	0.005
	Ge	4.006	0.770	3.351	0.018
3ORS-C	CNN1	4.087	0.436	4.291	0.011
	CNN2	4.035	0.00	4.040	0.00
Diamond	Ge	4.037	-0.78	3.302	0.003
	CNN1	4.168	0.00	4.248	0.00
Diamond	CNN2	3.927	0.00	4.390	0.00
	Ge	3.936	-0.757	3.268	0.00

clouds biased toward the C-atom side of diamond. Furthermore, the diagrams in Fig. 3 show that, during the electron transfer process, the Ge atoms lose electrons, while the C atoms gain electrons. This is explained by the higher electronegativity of C atoms (2.55) compared with Ge atoms (2.01) [26], which translates to C atoms being better at capturing electrons than Ge atoms. Table 3 summarizes the changes in the charges and magnetic moments of the Ge and C atoms before and after Ge adsorption, thus providing quantitative evidence to explain the bonding processes for the various diamond surfaces. For example, for the 1ORS diamond model, Table 3 shows that the charges of the C atoms increase, while the charge of the Ge atom decreases by 0.368e. Therefore, charge may transfer from Ge atoms to C atoms on the diamond surface. The magnitude of the magnetic moment is the difference between the spin-up and spin-down states in the density of states. The magnetic moments before and after Ge adsorption in Table 3 provide an indication of the bond strength between the Ge and C atoms and whether unpaired electrons remain after adsorption. The absolute values of the magnetic moments of the C and Ge atoms are reduced, which explains the strong interaction between the two in the differential charge diagram that results in the formation of a covalent bond. However, the magnetic moments of the C and Ge atoms after adsorption are not zero, indicating that both have unpaired electrons, which provides the basis for further bonding with the -CH group.

The adsorption of Ge atoms on the 2ORS diamond surface results in the charges of Ge atoms in 2ORS-CC, 2ORS-CO, and 2ORS-R being reduced by 0.588e, 0.688e, and 0.718e, respectively. These results represent an increase in charge reduction compared with the 1ORS diamond surface. The reason for this is that the Ge atoms in the 1ORS model engage in charge transfer with one C atom, while the Ge atoms in the 2ORS model are involved in charge transfer with two C atoms, which enables Ge atoms to be adsorbed on the diamond surface more stably. This also explains why the maximum adsorption energy of the 2ORS model is greater than that of the 1ORS model. The magnetic moment becomes zero following Ge adsorption, indicating the saturation of the extranuclear electrons belonging to the Ge atom and the two C atoms, which creates conditions conducive to the formation of vacancies in the subsequent stage of the diamond deposition process.

Following the adsorption of Ge atoms on the 3ORS diamond surface, the Ge atomic charge of 3ORS-C and 3ORS-R is reduced by 0.655e and 0.735e, respectively. This represents a considerable reduction in the Ge atomic charge compared with the 1ORS diamond surface. This is also the

reason that Ge atoms engaging in charge transfer with two C atoms. Comparing the 3ORS and 2ORS diamond surfaces reveals minimal changes in the degree of charge transfer. It is possible that the increase in the number of hydrogen-deficiency sites leads to an increase in the overall adsorption energy of the six high-symmetry sites; however, Ge atoms still form bonds with two C atoms on the 3ORS diamond surface. Therefore, when there are more than two hydrogen-deficiency sites, the impact on the extent of the charge transfer at the maximum adsorption energy site is small. Moreover, the magnetic moments of the Ge atoms on the 3ORS surface are non-zero, indicating the existence of unpaired electrons.

Upon comparing the differential charge diagrams with the changes before and after adsorption, the amount of charge at the maximum adsorption energy position on the hydrogen-free diamond surface is reduced by 0.668e, which corresponds to the main charge transfer to the two C atoms.

In addition to the surface with full hydrogen termination, for the diamond surfaces with different hydrogen terminations, the C atoms at the maximum adsorption energy positions form stable covalent bonds with Ge atoms. However, comparing the difference between the sum of the C and Ge atomic charges before and after adsorption shows that the total charge after adsorption is less than that before adsorption. Specifically, the total charge of the 1ORS, 2ORS-CC, 2ORS-CO, 2ORS-R, 3ORS-C, 3ORS-R, and Diamond surfaces is reduced by 0.148e, 0.141e, 0.358e, 0.546e, 0.427e, 0.526e, and 0.125e, respectively. This indicates that some of the electrons from the Ge atoms are not being transferred to the C atoms they are bonded to, but instead to other atoms in the vicinity of the Ge atoms. Consequently, the Ge atoms may be adsorbed on neighboring atoms.

3.3. Migration of germanium atoms on hydrogen-terminated and clean diamond surfaces

To study the adsorption stability and growth mechanisms of Ge atoms on diamond surfaces, we analyzed the process of Ge atom migration on the surface of (001) diamond under different hydrogen termination conditions. The NEB method [23] was used to calculate the energy change associated with the entire migration process (Fig. 4).

As shown in Fig. 4(a), Ge atoms on the 10RS diamond surface migrate from P5 to P2. Notably, the migration does not follow a straight line and is initially slightly biased toward the dimer opening position before switching toward the defect position. This is because there is no C–C bond in the ring opening of the dimer, which leaves large interatomic gaps. Although simple physical adsorption forms part of the Ge atom migration process, defects remain the most stable sites. The migration curve in Fig. 4(a) shows that no saddle point occurs during the migration from P5 to P2. However, in the process of moving from position III to position P2, a saddle point appears at position IV. This point represents the energy required for Ge atoms to avoid physical adsorption at the ring opening of the dimer during the migration process. Note that the minimum migration activation energy required to cross this saddle point is 0.051 eV. Migrating from P2 back to P5 requires a minimum migration activation energy of 0.925 eV, while an energy barrier of 2.179 eV must be overcome to release Ge atoms from the diamond surface at the P2 position.

Two migration paths, namely P4 to P1 and P5 to P1, were selected to investigate Ge migration on the 20RS-CC surface. As shown in Figs. 3(b) and (c), there are no saddle points in either migration path, suggesting that positions P4 and P1 can migrate easily to the most stable position (i.e., P1) on the 20RS-CC surface. The minimum migration activation energies required for Ge atoms to migrate from P1 to P4 and from P1 to P5 are 3.565 eV and 2.281 eV, respectively. To release Ge atoms from the diamond surface at P1, an energy barrier of 4.06 eV must be surmounted. Fig. 4(d) shows the migration path selected on the 20RS-CO surface, with no saddle point observed from P5 to P3. The minimum migration activation energy required for Ge atoms to migrate from P3 to

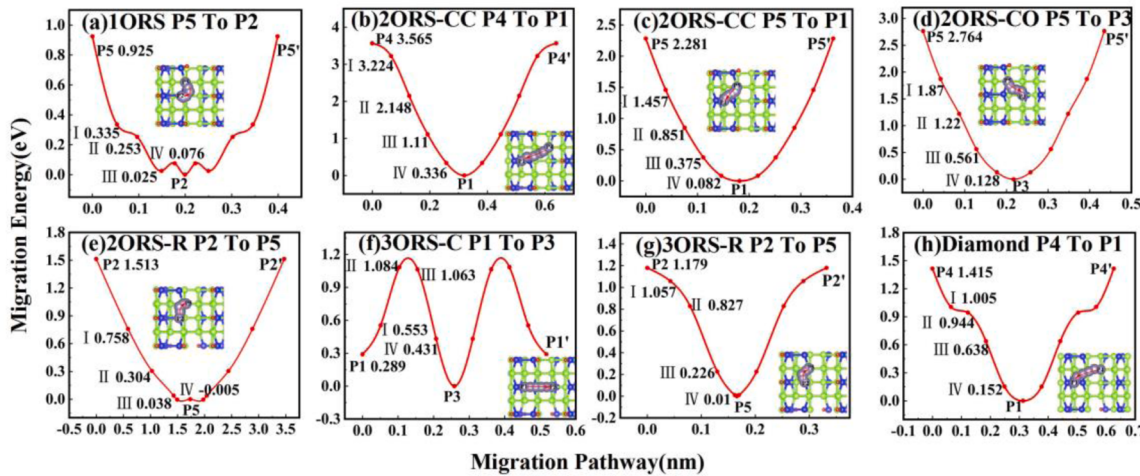


Fig. 4. Migration and diffusion of Ge atoms on various hydrogen-terminated diamond surfaces.

P5 is 2.764 eV, and an energy barrier of 4.162 eV must be overcome to migrate from P3 to the diamond surface. The migration path selected on the 2ORS-R surface (P2 to P5) is shown in Fig. 4(e). When Ge atoms migrate from P2 to P5, an energy of −0.005 eV appears at position IV. However, this does not mean that position IV is more stable than P5; rather, this energy is due to the spring force, which is also a factor for other migration positions when using the NEB method. The minimum migration activation energy required to migrate from position P5 to position P2 is 1.13 eV, while Ge atoms must cross an energy barrier of 4.075 eV to migrate from P5 to the diamond surface.

As shown in Fig. 4(f), Ge atoms migrate from P1 to P3 on the 3ORS-C surface. In this case, a saddle point, which is caused by the breaking of the bonds between the Ge atom and the surrounding C atoms during migration, is observed. A minimum migration activation energy of 0.759 eV is required to cross the saddle point. For Ge atoms to migrate from P3 back to the P1 position, a minimum migration activation energy of 1.084 eV is required, while an energy barrier of 3.314 eV must be surpassed for Ge atoms to migrate from the P3 position to the diamond surface. The migration path selected for the 3ORS-R surface, namely P2 to P5, is shown in Fig. 3(g). In this case, the activation energy does not need to be overcome for migration to occur. Nevertheless, Ge atoms must overcome a minimum migration activation energy of 1.179 eV to migrate from P5 back to P2, and Ge atoms migrating from P5 to the diamond surface require sufficient energy to cross a barrier of 4.306 eV.

For the hydrogen-free termination diamond surface, Ge atoms migrate from P4 to P1, as shown in Fig. 4(h). No saddle points appear during the migration process. Although an upward trend is observed at position II, the energy at this point is less than that at position I, and therefore position II is not a saddle point. The migration of Ge atoms from P1 back to P4 requires a minimum migration activation energy of 1.415 eV, while the migration of Ge atoms from P1 to the diamond surface requires an energy barrier of 3.516 eV to be surpassed.

The above analysis indicates that Ge atoms migrate to the most stable position on the surface of various types of diamond surfaces. In addition, migration from the diamond surface requires a large migration activation energy, which is difficult to achieve during normal experiments. Therefore, once Ge atoms are adsorbed on stable positions on the surface of different hydrogen-terminated diamonds, it is difficult to release them.

4. Conclusions

In this study, the first-principles method was applied to calculate and analyze the adsorption and migration processes of Ge atoms on the surfaces of different types of (001) diamond. Several conclusions can be

drawn from this analysis. First, because there are no active sites on the surface of perhydrogenated diamond, the adsorption energy is always negative, which prevents Ge atoms from being adsorbed on the perhydrogen-terminated diamond surface. However, hydrogen defects on the surface of non-perhydrogen-terminated diamond generate active sites, which results in the adsorption of Ge atoms. Moreover, as the degree of hydrogen deficiency on the surface of partially hydrogen-terminated diamond increases, the overall adsorption energy also increases. Overall, the hydrogen-free termination diamond surface absorbs Ge atoms most effectively, as demonstrated by the significantly larger minimum adsorption energy relative to other hydrogen-terminated diamond surfaces. The analysis of the differential charge density maps, Bader charge transfers, and magnetic moments reveals a significant charge shift in the differential charge diagrams. The Bader charge transfer and magnetic moment calculations provide quantitative support for these diagrams, showing that the transfer of charge between the Ge and C atoms results in the formation of a covalent bond. The sum of the charges of the Ge atoms and the C atoms to which they are bonded after adsorption is less than that before adsorption. After a Ge atom is adsorbed, some of its electrons are transferred to other neighboring atoms, which may result in the physical adsorption of the Ge atom by these neighboring atoms. During the migration process, the 3ORS-C diamond surface requires a minimum migration activation energy of 0.795 eV, with no saddle points occurring on the remaining surfaces during migration. Because the required migration activation energy is small, Ge atoms can easily reach a stable position during the CVD process. By calculating the energy barrier at the most stable position on the diamond surface, it is clear that releasing Ge atoms that are adsorbed on the most stable position on the diamond surface is extremely difficult. Combined, the results of this study demonstrate that active sites on the diamond surface are beneficial for Ge doping.

CRediT authorship contribution statement

Xin Tan: Conceptualization, Methodology, Project administration, Formal analysis, Writing – original draft, Writing – review & editing, Supervision, Project administration. **Wei Shao:** Conceptualization, Software, Formal analysis, Data curation, Writing – original draft, Writing – review & editing, Visualization. **Xiyu Ma:** Formal analysis, Software. **Zanqing He:** Formal analysis. **Bochen Zhang:** Formal analysis, Software. **Chengbin Chen:** Formal analysis, Software. **Yuan Ren:** Formal analysis. **Shiyang Sun:** Formal analysis.

Declaration of Competing Interest

The authors declare that they have no known competing financial interests or personal relationships that could have appeared to influence the work reported in this paper.

Acknowledgments

This work is supported by the National Natural Science Foundation of China (61765012), Natural Science Foundation of Inner Mongolia (2019MS05008, 2019LH05003), National Key Research and Development Program of China (2017YFF0207200), and Inner Mongolia Autonomous Region Science and Technology Innovation Guidance Project (2017CXYD-2, KCBJ2018031).

References

- [1] D. Friederike, G. Heiko, P. Michael, T. Ladji, Wear mechanisms of diamond-coated tools, *Surf. Coat. Technol.* 142 (2001) 674–680.
- [2] M.V.G. Dutt, L. Childress, L. Jiang, E. Togan, J. Maze, F. Jelezko, A.S. Zibrov, P. R. Hemmer, M.D. Lukin, Quantum register based on individual electronic and nuclear spin qubits in diamond, *Science* 316 (2007) 1312–1316.
- [3] K. Ohashi, T. Rosskopf, H. Watanabe, M. Lorentz, Y. Tao, R. Hauer, S. Tomizawa, T. Ishikawa, J. Ishi-Hayase, S. Shikata, C.L. Degen, K.M. Itoh, Negatively charged nitrogen-vacancy centers in a 5 nm thin 12C diamond film, *Nano Lett.* 13 (2013) 4733–4738.
- [4] G. Balasubramanian, P. Neumann, D. Twitchen, M. Markham, R. Kolesov, N. Mizuochi, J. Isoya, J. Achard, J. Beck, J. Tissler, V. Jacques, P.R. Hemmer, F. Jelezko, J. Wrachtrup, Ultralong spin coherence time in isotopically engineered diamond, *Nat. Mater.* 8 (2009) 383–387.
- [5] M. Leifgen, T. Schröder, F. Gädke, R. Riemann, V. Métillon, E. Neu, C. Hepp, C. Arend, C. Becher, K. Lauritsen, O. Benson, Evaluation of nitrogen- and silicon-vacancy defect centres as single photon sources in quantum key distribution, *New J. Phys.* 16 (2013), 023021.
- [6] M.K. Bhaskar, D. Sukachev, A. Sipahigil, R.E. Evans, M.J. Burek, C.T. Nguyen, L. J. Rogers, P. Siyushev, M.H. Metsch, H. Park, F. Jelezko, M. Loncar, M.D. Lukin, Quantum nonlinear optics with a germanium-vacancy color center in a nanoscale diamond waveguide, *Phys. Rev. Lett.* 118 (2017), 223603.
- [7] T.T. Trong, B. Regan, E.A. Ekimov, Z. Mu, Y. Zhou, W. Gao, P. Narang, A. S. Solntsev, M. Toth, I. Aharonovich, C. Bradac, Anti-stokes excitation of solid-state quantum emitters for nanoscale thermometry, *Sci. Adv.* 5 (2019) eaav9180.
- [8] T. Iwasaki, F. Ishibashi, Y. Miyamoto, Y. Doi, S. Kobayashi, T. Miyazaki, K. Tahara, K.D. Jahnke, L.J. Rogers, B. Naydenov, F. Jelezko, S. Yamasaki, S. Nagamachi, T. Inubushi, N. Mizuochi, M. Hatano, Germanium-vacancy single color centers in diamond, *Sci. Rep.* 5 (2015) 12882.
- [9] K.D. Jahnke, A. Sipahigil, M.J. Binder, M.W. Doherty, M. Metsch, L.J. Rogers, N. B. Manson, M.D. Lukin, F. Jelezko, Electron-phonon processes of the silicon-vacancy centre in diamond, *New J. Phys.* 17 (2015), 043011.
- [10] T. Iwasaki, F. Ishibashi, Y. Miyamoto, Y. Doi, S. Kobayashi, T. Miyazaki, K. Tahara, K.D. Jahnke, L.J. Rogers, B. Naydenov, F. Jelezko, S. Yamasaki, S. Nagamachi, T. Inubushi, N. Mizuochi, M. Hatano, Germanium-vacancy single color centers in diamond, *Sci. Rep.* 5 (2015) 12882.
- [11] J.W. Fan, I. Cojocaru, J. Becker, A. Alajlan, M. Alkahtani, Germanium-vacancy color center in diamond as a non-invasive temperature sensor, *ACS Photonics* 5 (2017).
- [12] J.E. Butler, Y.A. Mankelevich, A. Cheesman, J. Ma, M.N. R. Ashfold, Understanding the chemical vapor deposition of diamond: recent progress, *J. Phys. Condens. Matter* 21 (2009), 364201.
- [13] A.M. Zaitsev, Vibronic spectra of impurity-related optical centers in diamond, *Phys. Rev. B* 61 (2000) 12909–12922.
- [14] A. Trycz, B. Regan, M. Kianinia, K. Bray, M. Toth, I. Aharonovich, Bottom up engineering of single crystal diamond membranes with germanium vacancy color centers, *Opt. Mater. Express* 9 (2019) 4708.
- [15] G. Kresse, J. Hafner, Ab initio molecular dynamics for liquid metals, *Phys. Rev. A* 47 (1995) 222–229.
- [16] G. Kresse, J. Furthmüller, Efficient iterative schemes for ab initio total-energy calculations using a plane-wave basis set, *Phys. Rev. B* 54 (1996) 11169.
- [17] G. Kresse, J. Furthmüller, Efficiency of ab-initio total energy calculations for metals and semiconductors using a plane-wave basis set, *Comp. Mater. Sci.* 6 (1996) 15–50.
- [18] P. Blöchl, Projector augmented-wave method, *Phys. Rev. B* 50 (1994) 17953–17979.
- [19] G. Kresse, D. Joubert, From ultrasoft pseudopotentials to the projector augmented-wave method, *Phys. Rev. B* 59 (1999) 1758–1775.
- [20] J.P. Perdew, K. Burke, M. Ernzerhof, Generalized gradient approximation made simple, *Phys. Rev. Lett.* 77 (1996) 3865–3868.
- [21] J.P. Perdew, A. Ruzsinszky, G.I. Csonka, O.A. Vydrov, G.E. Scuseria, L. A. Constantin, X. Zhou, K. Burke, Restoring the density-gradient expansion for exchange in solids and surfaces, *Phys. Rev. Lett.* 100 (2008), 136406.
- [22] H. Monkhorst, J.D. Pack, Special points for Brillouin-zone integrations, *Phys. Rev. B* 13 (1976) 5188–5192.
- [23] G. Henkelman, G. Jónasson, H. Jónsson, Methods for finding saddle points and minimum energy paths, in: S.D. Schwartz (Ed.), *Progress in Theoretical Chemistry and Physics* 5, Kluwer Academic Publisher, New York/Boston, USA, 2021, pp. 269–302.
- [24] X. Liu, H. Wang, P. Lu, Y. Ren, X. Tan, S. Sun, H. Jia, First principles calculations of the adsorption and migration behaviors of N atoms on the H-terminated diamond (001) surface, *Appl. Surf. Sci.* 463 (2019) 668–678.
- [25] X. Liu, S. Zhang, Y. Jiang, Y. Ren, Interface structure of nanodiamond composite films: first-principles studies, *J. Alloys Compd.* 599 (2014) 183–187, 3.
- [26] C. Kittel, H.Y. Fan, Introduction to solid state physics, *Phys. Today* 10 (6) (1957) 43–44.
- [27] H.L. Yu, X.D. Deng, G. Li, X.C. Lai, D.Q. Meng, Strong and weak adsorption of CO₂ on PuO₂(1 1 0) surfaces from first principles calculations, *Appl. Surf. Sci.* 316 (2014) 625–631.